FISEVIER

Contents lists available at ScienceDirect

## International Journal of Mass Spectrometry

journal homepage: www.elsevier.com/locate/ijms



# Simplified coaxial ion trap: Simulation-based geometry optimization, unidirectional ejection, and trapping conditions



Radhya W. Gamage <sup>a</sup>, Praneeth M. Hettikankanange <sup>a</sup>, Kyle D. Lyman <sup>b</sup>, Daniel E. Austin <sup>a, \*</sup>, Nicholas R. Taylor <sup>b</sup>

#### ARTICLE INFO

Article history:
Received 30 September 2021
Received in revised form
25 December 2021
Accepted 10 January 2022
Available online 18 January 2022

Keywords:
Toroidal ion trap
Coaxial ion trap
SIMION
Mass spectrometry
Unidirectional ejection
Radial trapping

### ABSTRACT

We have simulated the design and performance of the simplified coaxial ion trap – a dual ion trap mass spectrometer consisting of an outer simplified toroidal trap and an inner cylindrical trap. The device can perform tandem mass analysis by initially trapping ions in the toroidal region, and then transferring ions mass-selectively to the cylindrical region where they can be fragmented, isolated, and mass-scanned. The key benefit of the coaxial trap is the ability to store and retain the original ion population in the toroidal region while tandem mass analysis is being done in the cylindrical region for a selected mass. This study models a miniaturized simplified coaxial ion trap using the ion trajectory simulation software, SIMION, and characterizes its performance in terms of mass resolution and selectivity of transfer from toroidal to cylindrical regions, ion ejection direction from the toroidal trap, and trapping efficiency in the cylindrical trap. Mass resolution was maximized with a slightly positive octopole term in the toroidal trapping region, and the desired inward radial ejection of ions was achieved with a positive hexapole term. We demonstrate the possibility to obtain an optimized electric field for a given aspect ratio of the toroidal trap by varying only three geometric parameters. Simulated mass resolution from the optimized geometry was 0.3 Da for aspect ratio 8. The trapping efficiency was found to be affected by RF and AC voltages, RF phase, as well as the pressure. A mismatch between the kinetic energy of transferred ions and the RF phase in the cylindrical trap at the time of transfer was found to account for most of the ion loss during transfer. The intricate dependence of trapping efficiency on a number of operational variables was found to lead to trade-offs between itself and other operational parameters such as mass resolution and transfer efficiency. The results demonstrate successful operation of the simplified coaxial trap and reveal the geometric and operational constraints to be considered in its operation.

© 2022 Elsevier B.V. All rights reserved.

## 1. Introduction

Miniaturized ion traps have become the preferred mass analyzer for applications requiring in-field chemical analysis [1,2]. The compact size, low power consumption, and reduced pressure requirements make miniaturized ion traps easily incorporated into portable chemical analysis systems. The reduced pressure requirements and rapid mass scan capabilities make ion traps an ideal mass analyzer when coupled to front end chromatographic systems, facilitating numerous analytical applications ranging from in-field analysis of biological samples to space exploration [3–6].

Moreover, ion traps are capable of tandem-in-time mass analysis (MS<sup>n</sup>), providing a distinct analytical advantage in the analysis of in-field samples possessing a complex chemical matrix.

Quadrupole ion traps (QIT) and cylindrical ion traps (CIT) function by focusing all trapped ions into a small spheroidal volume at the center of the trap. While functional in its purpose of ion storage and mass analysis, it was soon realized that the Coulombic repulsion from a large number of like charged ions within a small trapping volume would deteriorate the devices performance, a phenomenon known as space charge effects which is directly related to the trapping capacity of the device [7]. Space charge effects are exacerbated when QIT and CIT devices are miniaturized, limiting their analytical utility. Indeed, increasing the trapping capacity of miniaturized ion traps would be required to improve the analytical performance of portable chemical analysis systems. Since

<sup>&</sup>lt;sup>a</sup> Department of Chemistry and Biochemistry, Brigham Young University, Provo, UT, USA

<sup>&</sup>lt;sup>b</sup> Department of Mechanical and Aerospace Engineering, Western Michigan University, Kalamazoo, MI, USA

<sup>\*</sup> Corresponding author.

E-mail address: austin@chem.byu.edu (D.E. Austin).

the introduction of the QIT and CIT, a number of ion trap geometries have been developed to resolve the limiting trapping capacity issue. The linear ion trap (LIT) extends the trapping volume by elongating the trapping dimension to a linear region [8,9]. The rectilinear ion trap (RIT) was subsequently developed as a simplified version of the LIT and facilitated easy fabrication when miniaturized [10]. Ring-shaped ion traps have also been developed; however, they originally functioned as ion storage devices for studies of phase transitions, structures, and spectroscopic applications [11–13]. In 2001, Lammert et al. developed a toroidal ion trap (TorIT) for the purpose of mass analysis [14]. The prototype TorIT consisted of a symmetric ring-shaped trapping region with axial ion ejection and detection. While functional, it was discovered that the curvature of the electrodes created an electric field which adversely impacted the device performance. The second TorlT version consisted of asymmetric electrodes which accounted for the toroidal curvature and demonstrated a significant improvement in analytical performance. In 2012, Taylor et al. reported the first instance of a simplified toroidal ion trap (STorIT) which consisted of cylindrical electrodes [15]. The STorIT reported a mass resolution of  $\Delta m = 0.32$ and demonstrated tandem mass analysis capabilities.

A key advantage possessed by LIT, RIT, TorIT, and STorIT devices is the decoupling of the characteristic trapping dimension from the ion trapping capacity. An ion trap's aspect ratio, a parameter defined as the ratio between the extended trapping dimension and the characteristic trapping dimension, has become an important parameter in the evaluation of TorIT and STorIT devices. Despite the reduced characteristic trapping dimension as a consequence of miniaturization, the ion trapping capacity can remain unaffected by simply increasing the trapping dimension, yielding a high aspect ratio trap. Recently, Hettikankanange et al. studied the effect of aspect ratio on both an asymmetric TorIT and STorIT [16]. Examining aspect ratios from 1.86 to infinity, it was found that certain key device metrics were most sensitive to changes in aspect ratio between 1.86 and 10.

Ion traps of toroidal geometry conveniently lend themselves to form a dual ion trap with a second ion trap placed in the hollow center of the toroidal trap, resulting in a coaxial ion trap. The first instance of a coaxial ion trap was reported by Austin et al. and was formed with concentric rings lithographically printed on two parallel ceramic plates, creating an outer toroidal trapping region and a quadrupole trapping region at the center [17]. The lithographically patterned coaxial ion trap demonstrated good mass resolution and sensitivity; however, the ion transfer from toroidal to quadrupole regions lacked mass selectivity.

In this work, we introduce the simplified coaxial ion trap consisting of an outer STorIT and an inner CIT. Ions are initially trapped and stored within the STorIT, following which a chosen m/z ratio is selectively transferred to the CIT. The transferred ions trapped within the CIT can be analyzed directly or undergo  $MS^n$  analysis. Since the original ion population remains in the STorIT while  $MS^n$  mass analysis is being performed in the CIT, multiple  $MS^n$  analyses can be performed on multiple masses stored within the STorIT without having to repopulate the STorIT, increasing analytical efficiency and sample utilization. This is in contrast with the conventional mode of  $MS^n$  mass analysis with a single ion trap, where the targeted mass is first isolated by the elimination of other masses from the trap.

Coaxial traps of similar design to that of the present study have been the focus of a few simulation studies in the recent past. Yu et al. demonstrated some aspects of operation including radial ejection of ions from the toroidal region and trapping of radially injected ions in the cylindrical trap [18]. However, seamless transfer and trapping was not demonstrated. Hai-Yung et al. addressed the aspect of ion ejection direction by adjusting the shape of toroidal

electrodes [19]. While these previous studies demonstrated coaxial ion trap operation, further geometry optimization and comprehensive characterization is still required.

The present study focuses on understanding the performance of a simplified coaxial ion trap with aspect ratios 2.2, 3, and 8. The parameters most critical to analytical performance include mass resolution and mass selectivity of ion transfer from toroidal to cylindrical regions, ion ejection direction from the STorIT, transfer efficiency to the cylindrical region, and trapping efficiency in the CIT. These functionalities have not been fully treated in previous studies and require a comprehensive examination with respect to aspect ratio and electrode geometry. Results from this study can be utilized to optimize the analytical performance of a simplified coaxial ion trap within a portable chemical analysis system.

#### 2. Method

The geometric cross-section of the coaxial ion trap studied here is shown in Fig. 1. To study the effect of geometric parameters, electrode geometries with incremental changes to w, h, and  $z_0$  were constructed separately for the aspect ratios 2.2, 3, 8. All simulations were performed with SIMION 8.1 ion trajectory simulation software (Scientific Instrument Services, Ringoes, NJ).

The electric field was characterized by recording the radial potential and fitting to an  $8^{th}$  order polynomial. The polynomial coefficients obtained represent the magnitudes of the multipole terms. The multipoles were calculated by considering the outward direction from the trap center as the positive radial direction. Higher-order field contributions were then obtained by expressing the multipoles as percentages of the quadrupole ( $A_2$ ) term. This mathematical representation of the toroidal electric field, however, is only an approximation because the absence of a continuous and differentiable electric field at the axis of rotation of the toroidal trap signifies that the conditions of the Laplace equation are not met. Moreover, all higher-order terms may not be centered around the same radial distance.

## 3. Results and discussion

## 3.1. STorIT: geometry and higher order multipole components

Initial analysis of the coaxial ion trap involved examination of the STorIT in the absence of the CIT. A comprehensive analysis has been conducted on the relationship between electrode geometry and nonlinear electric field components, as well as the effect of the above on mass resolution and ejection direction. With respect to the STorIT, three geometric variables are used to vary the electric field for a given aspect ratio and are noted in Fig. 1: the width of  $AC_{Tor} = w$ , the  $RF_{Tor}$  and ejection slit gap = h, and the stretching of the  $RF_{Tor}$  electrodes =  $z_0$ . The ejection slit width remained constant at 1.2 mm throughout this study. The degree of electrode curvature is dictated by the trap's aspect ratio and is another important parameter affecting the magnitude of the higher-order multipole components. Aspect ratios of 2.2, 3, and 8 are considered here with  $r_0 = 5$  mm maintained constant and the value of R adjusted to achieve the desired aspect ratio. A recent investigation into the impact of aspect ratios on higher order multipole terms concluded that this range of aspect ratios possess the greatest impact on a STorIT electric field and analytical performance [16].

The performance of the STorIT was evaluated by simulating the mass resolution of ions ejected using a reverse scan with AC resonant ejection. Initially the toroidal region was populated with 600 ions with a m/z = 90 and allowed to cool for 1 ms. The hard sphere collision model (HS1) was used to model the system with a pressure of 1 mTorr and a temperature 298 K. The collision cross-section

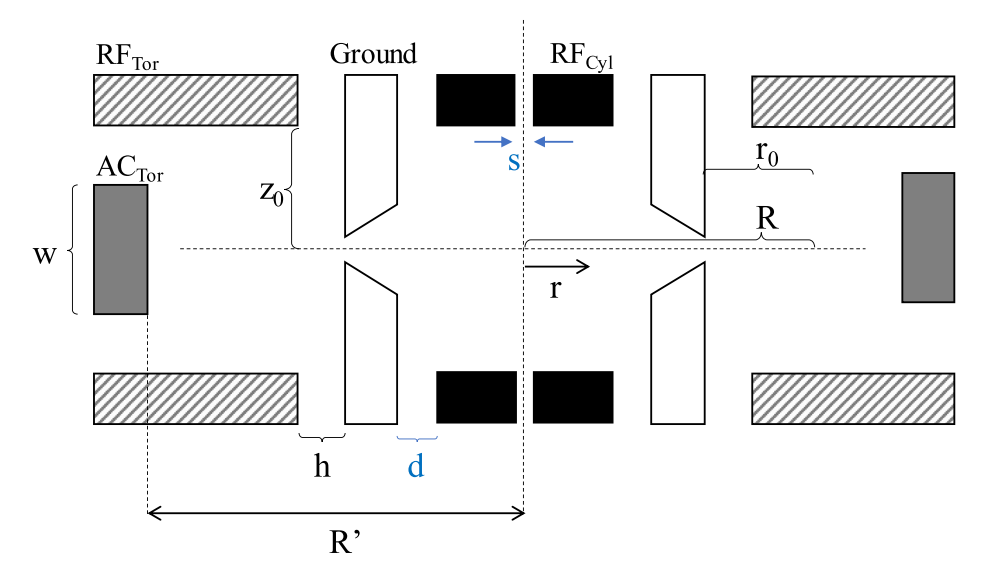


**Fig. 1.** Illustration of the simplified coaxial ion trap with an aspect ratio  $R/r_0 = 3$ .

 $(\sigma)$  between the ions and helium gas was calculated using the classic hard sphere collision cross-section formula for two particles,  $\sigma_{AB}=\pi(r_A+r_B)^2,$  where  $r_A$  and  $r_B$  are the hard sphere radii of the two elastically colliding particles. The radius of the m/z=90 ion was taken as equal to that of a toluene molecule yielding  $\sigma_{AB}=5.6\times10^{-19}~\text{m}^2$  [20]. During the ion populating and cooling process, a 1.5 MHz potential applied to RF<sub>Tor</sub> electrodes was maintained at  $285V_{(0-p)}$  with a 5 V DC offset. After ion cooling, the RF potential was ramped at 5 kDa/s. Resonance ejection was achieved by applying 3  $V_{(0-p)}$  potential at 270.5 kHz to AC<sub>Tor</sub>. Throughout this study the RF<sub>Tor</sub> voltages were adjusted to ensure ion ejection occurred at  $\beta=0.36$  for all geometries and aspect ratios examined, unless otherwise stated. Moreover, AC voltages were also adjusted to ensure all ions received enough energy to be ejected.

Mass spectral peaks were constructed by converting the temporal distribution of ion ejection to peak width. This was achieved by calculating the RF amplitude at the time of ion ejection. The resulting distribution of RF amplitudes was linearly mass calibrated by assigning the mode of the distribution to the target mass (m/z=90) and rounding to the nearest 0.1 Da. The simulated spectral peak was constructed by plotting the ion count obtained vs. m/z.

Fig. 2 summarizes the response of the electric field and mass resolution to variations in the AC electrode width (w), gap between ground and RF electrodes (h), and the axial trapping dimension (z<sub>0</sub>).

Mass resolution deteriorates as the octopole term becomes larger, and is optimal at low positive octopole values with  $\Delta m \sim 0.3$  Da. This result is quantitatively consistent with previous reported simulation studies on other types of ion traps such as QIT, LIT, RIT, and CIT, as well as experimental work on the STorIT, where a slightly positive  $A_4$  term was found to yield the best mass resolution [10,15,21–23]. Any correlation between  $\Delta m$  and the  $A_3, A_5,$  or  $A_6$  terms was found to be negligible. An example of mass spectra constructed from the simulations described above at an aspect ratio of 8 is shown in Fig. 3.

## 3.2. STorIT: transfer Selectivity with selective resonance ejection

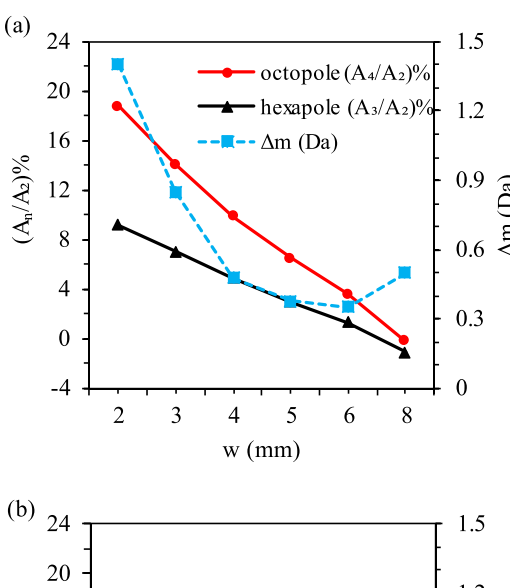
In coaxial ion trap operation, a targeted ion or m/z value is selectively transferred from the STorIT to the CIT using resonant ejection while maintaining a fixed RF voltage. The examination of transfer selectivity with resonance ejection utilized STorIT geometric values of h=1 mm, w=6 mm, and  $z_0=5$  mm which results

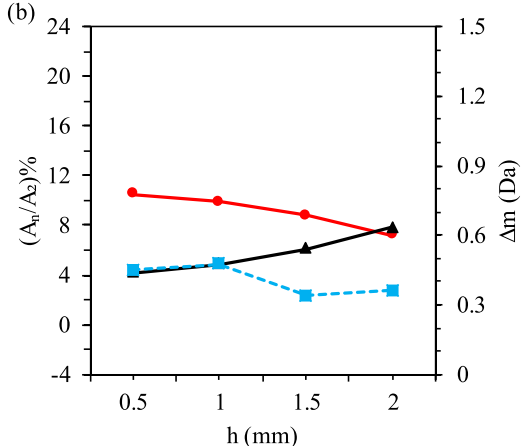
in  $A_3 = 1.3\%$ ,  $A_4 = 3.6\%$ ,  $A_5 = 3.6\%$ , and  $A_6 = -9.2\%$ . For these simulations, 100 ions with masses ranging from m/z = 87-93 in 0.5 Da increments for a total 1300 ions were introduced to the STorIT region. Initially the ions were allowed to cool for 1 ms at an applied potential of RF<sub>Tor</sub> = 278.9  $V_{(0-p)}$  at 1.5 MHz. Following ion cooling, a potential was applied to AC<sub>Tor</sub> with a frequency of 270.5 kHz which selectively targeted the m/z = 90 ions for ejection into the CIT. The secular frequency of the m/z = 90 ion was determined from the fast Fourier transform (FFT) of its position coordinates. This provided a close approximation of the resonant AC frequency. As with previous simulations, the CIT is not considered. Results from these simulations are shown in Fig. 4 for three different AC<sub>Tor</sub> potentials. Depending on the magnitude of the AC<sub>Tor</sub>, a mass range of approximately ±3 Da in the vicinity of the targeted ion respond to the resonant AC signal and are ejected. This suggests that the low transfer selectivity may be an inherent shortcoming of this mode of operation combined with the currently examined higher-order field components. It should be noted that the coaxial ion trap with lithographically patterned electrode rings, which was operated in the same mode described here, lacked mass selectivity in transferring ions from outer toroidal to inner quadrupole regions; a likely result of the higher-order field configuration [17]. In the current design, fine-tuning the amplitude and duration of the AC<sub>Tor</sub> signal brought about some improvement. Limiting the AC<sub>Tor</sub> signal to 1 ms and 3  $V_{(0-p)}$  narrowed the mass range.

Moreover, the potential applied to  $AC_{Tor}$  impacts the mass resolution of the STorIT (not shown). At low amplitudes of AC, of around 1–2  $V_{(0-p)}$ , ions were seen to eject over a longer period of time, likely a result of the octopole field causing the ions to oscillate between resonant and non-resonant conditions as its radial amplitude oscillates [24]. This explains the role of the higher amplitude AC which allows the target ions to absorb energy and eject rapidly over a shorter time, before falling out of resonance, resulting in better mass resolution. On the other hand, high AC voltages of 4–5  $V_{(0-p)}$  and above resulted in ion ejection efficiency near 100%; however, transfer selectivity deteriorates to  $\pm 2$  Da as was shown in Fig. 4.

## 3.3. STorIT: unidirectional ion ejection

An important aspect of the proposed coaxial ion trap is the ability of the STorIT to transfer ions into the CIT; thus, the direction of ion ejection from the STorIT region is a prerequisite for successful





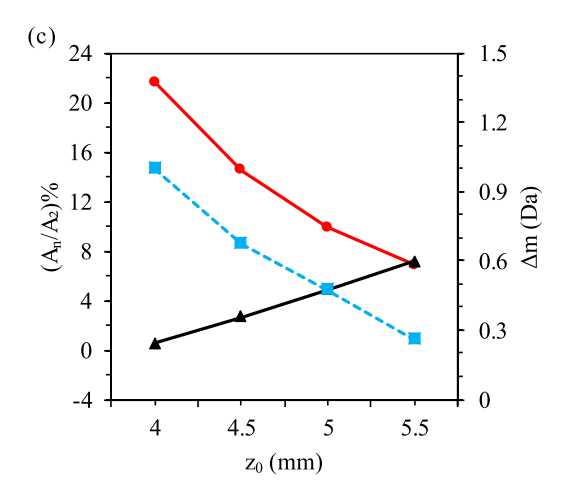


**Fig. 2.** Plots of the variation of electric field multipoles (solid lines) and mass resolution (dotted line) with geometric parameters for aspect ratio 8. Mass resolution,  $\Delta m$  (Da) was measured as full width at half maximum (FWHM) of the peak. (a) h=1 mm,  $z_0=5$  mm (b) w=4 mm,  $z_0=5$  mm (c) w=4 mm, w=4

operation. For the lowest aspect ratio of 2.2, it was observed that a significant fraction of ions eject radially outwards, impacting on the surface of the  $AC_{Tor}$  electrode. A study of this ion behavior reveals that the radial outward ejection correlates with the hexapole term (Fig. 5). At higher aspect ratios, where all of the geometries have a positive or only slightly negative  $A_3$  term, display radial inward ejection as desired. As the  $A_3$  term becomes more negative in aspect ratio 2.2, more ions tend to eject outwards. Since the hexapole term

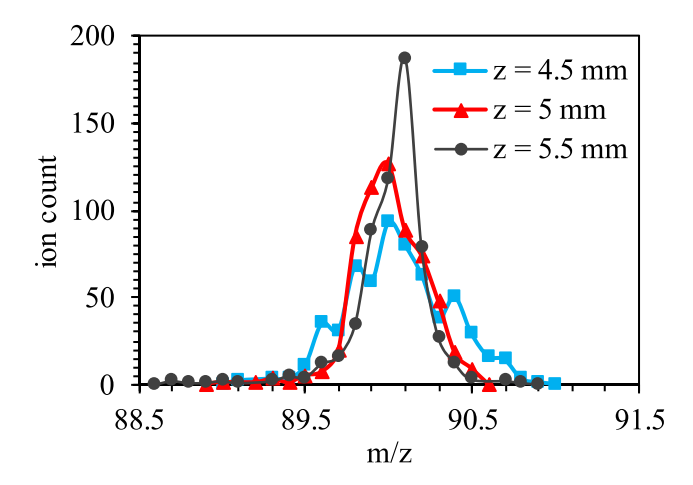


**Fig. 3.** Simulated spectra showing the variation of resolution with multipoles with RF ramp. Octopole  $(A_4)$  terms are 14.5%, 9.9%, and 6.9% for axial trapping dimensions of 4.5 mm, 5 mm, and 5.5 mm respectively. Each spectrum was obtained with 600 ions. The mass spectra shown are for w=4 mm, h=1 mm, and an aspect ratio of 8. Error in the data (not shown) is a function of the square root of the number of ions.

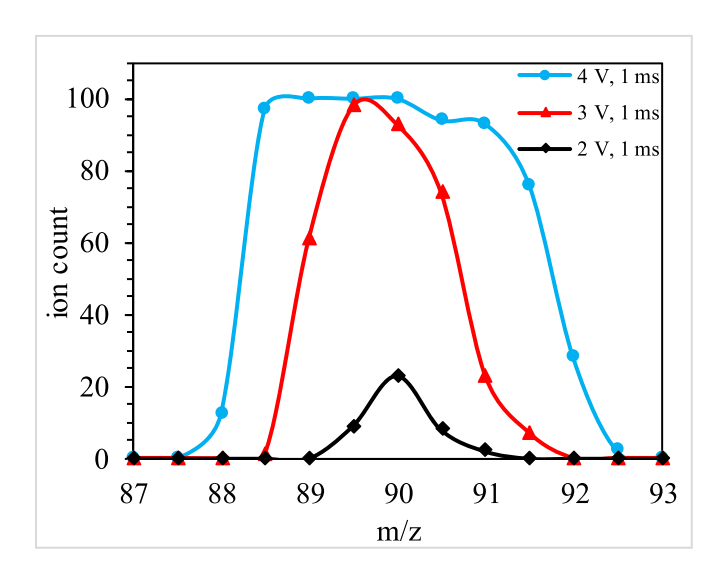


**Fig. 4.** Transfer selectivity of resonant ion ejection from the STorIT with an aspect ratio 8. Each point represents the number of ions transferred out of the STorIT out of 100 ions per mass. Error in the data (not shown) is a function of the square root of the number of ions.

represents the radial asymmetry of the trapping field, it is reasonable that as the direction of the field asymmetry switches from negative to positive, i.e. outward to inward, the direction of ion ejection would respond similarly.

The potential applied to  $AC_{Tor}$  excites the ions radially; however, significant axial excitation of ions could be seen as  $\beta$  values exceeded 0.4. These ions impact on the  $RF_{Tor}$  electrodes or, at lower degrees of axial excitation, fail to pass through the ejection slit and impact on the barrel electrode. This apparent coupling of radial and axial motions is readily explained by the fact that radial and axial secular frequencies approach each other with increasing  $\beta$ . The application of a larger DC offset increases the difference between radial and axial secular frequencies and thereby reduces undesirable axial excitations. This observed undesirable axial excitation is the reason why  $RF_{Tor}$  was adjusted to maintain a value of  $\beta=0.175$  for all geometries and aspect ratios examined.

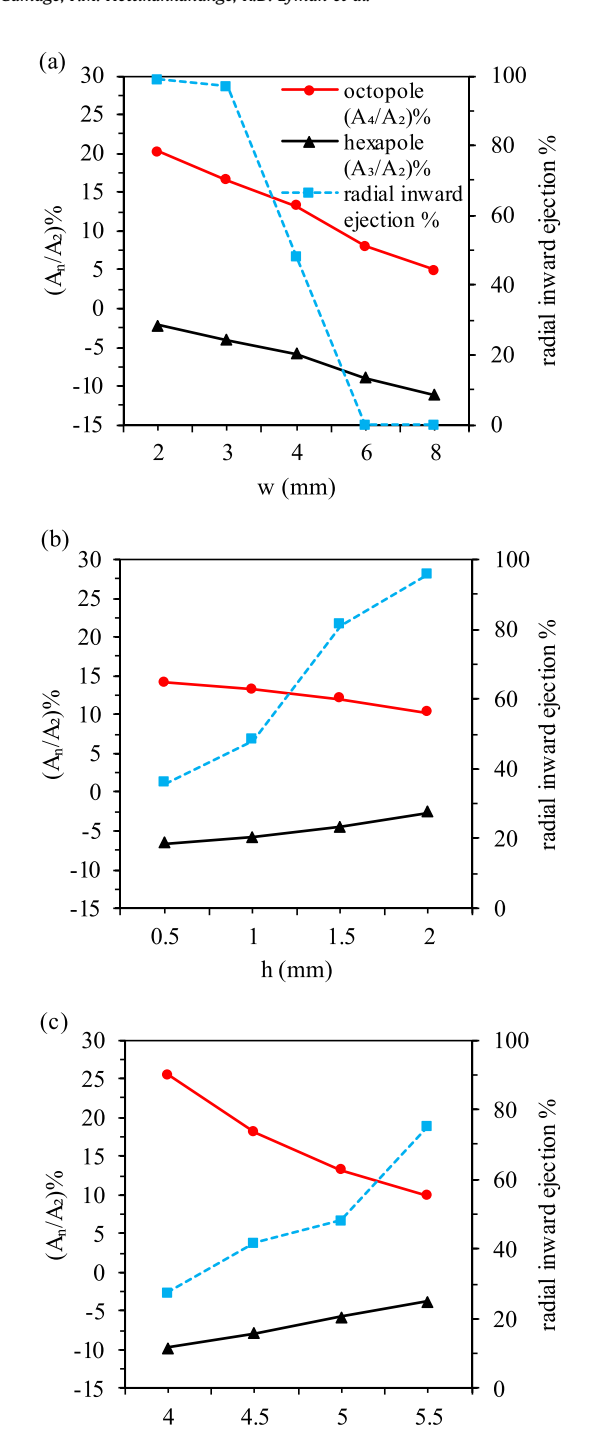


**Fig. 5.** Variation of inward radial ejection percentage with geometric parameters in aspect ratio 2.2. The solid lines represent the variation in hexapole and octopole terms. The dashed lines represent the variation of inward radial ejection at  $\beta=0.175$ . (a)  $h=1\ mm,\ z_0=5\ mm$  (b)  $w=4\ mm,\ z_0=5\ mm$  (c)  $w=4\ mm,\ h=1\ mm$ .

 $z_0 (mm)$ 

## 3.4. The coaxial ion trap: geometry considerations

The greatest contributions to performance are made by the hexapole and octopole terms, affecting ion ejection direction and mass resolution, respectively. As shown in Fig. 2,  $A_3$  and  $A_4$  terms respond similarly to changes to the w parameter; however, they have the opposite response to changes in h and  $z_0$ . Therefore, it becomes possible to manipulate electrode geometry to achieve

optimal conditions for a given aspect ratio. With this approach, we obtained an optimized electrode geometry for aspect ratio 3 which was used in the subsequent simplified coaxial ion trap simulations. Here, the STorIT dimensions were  $w=5\,$  mm,  $h=2\,$  mm, and  $z_0=5.5\,$  mm, while the CIT was  $z_0=5.5\,$  mm,  $r_0=7\,$  mm, with an end-cap hole diameter,  $s=2\,$  mm, and  $d=1.8\,$  mm in keeping with the -10% compensation rule [25]. Given that the electric field of the CIT was consistent with the said rule in the presence of the toroidal electrodes, we expect that the performance of the CIT would not be affected by the STorIT voltages.

## 3.5. Coaxial ion trap operation

The operation of the coaxial ion trap was examined by populating the STorIT with ions, mass selectively transferring ions to the CIT, and trapping the transferred ions in the CIT. Since SIMION is not capable of performing ion fragmentation via collisionally induced dissociation (CID), trapping and mass selective ejection of fragment ions from the CIT were performed separately.

A challenging aspect of the proposed coaxial ion trap operation is the presence of an RF barrier between the STorIT and CIT regions which must be overcome for successful transfer of ions. For a given combination of RF $_{\text{Tor}}$  voltage and pressure, there is a minimum kinetic energy that ions require to escape the pseudopotential well. This kinetic energy, provided by the AC voltage, also needs to be sufficiently low to allow the ions to be decelerated and trapped in the CIT region.

Depending on their kinetic energy, ions display one of three behaviors during transfer from toroidal to cylindrical regions: 1) enter the cylindrical region and get trapped, 2) enter the cylindrical trap and get reflected back towards the injection slit, or 3) traverse the cylindrical region and emerge on the opposite side of the toroidal region or collide with the barrel electrode. These three behaviors occur at varying degrees regardless of the m/z of the ion falling within the stability region of the CIT. The latter two outcomes, which account for ion losses during transfer, are also common to ion injection in a 3D QIT [26]. Past studies have shown the radial injection efficiency of ions to a 3D QIT to be around 5% [26,27]. One approach to improving the ion injection efficiency of the 3D QIT was to match the RF phase to the ions kinetic energy [7,26,28,29]. In the case of LIT's, 100% trapping efficiency has been shown with axial injection of ions. The longer path length over which ions may be collisionally decelerated as well as the lack of an RF barrier along the injection axis facilitate trapping in the LIT [30]. In the dual-LIT design presented by Li et al., ions were transferred axially with a mass-selective transfer efficiency of 55% [31].

## 3.6. RF phase vs. ion kinetic energy

A study of ion kinetic energy and absolute RF phase of the CIT was conducted on ions with m/z=219 injected into the CIT in order to examine the fate of ions with respect to the three outcomes described above. The RF frequency on the STorIT and CIT were kept at 1.5 MHz while the RF<sub>Tor</sub> and RF<sub>Cyl</sub> potentials were maintained at 575 V<sub>(0-p)</sub> and 1050 V<sub>(0-p)</sub> respectively. A DC offset of 5 V was applied to RF<sub>Tor</sub>. The RF phase angle of the CIT leads that of the STorIT by 150°, as indicated on the secondary horizontal axis. An AC voltage of 3 V<sub>(0-p)</sub> at 108 kHz was applied for 100  $\mu$ s, maintaining  $\beta=0.144$ . The pressure was maintained at 3.75 mTorr. Fig. 6 shows the range of RF phase over which ions enter the CIT and the distribution in ion kinetic energy at the point of entry.

At a first glance, it is apparent that no ions transfer from the STorIT to the CIT between  $90^{\circ}$  and  $230^{\circ}$  absolute phase angle of CIT RF voltage, (i.e.  $-60^{\circ}-80^{\circ}$  of the RF phase of the STorIT). Over this range, the RF barrier of the STorIT is on the rise, thus, the ion

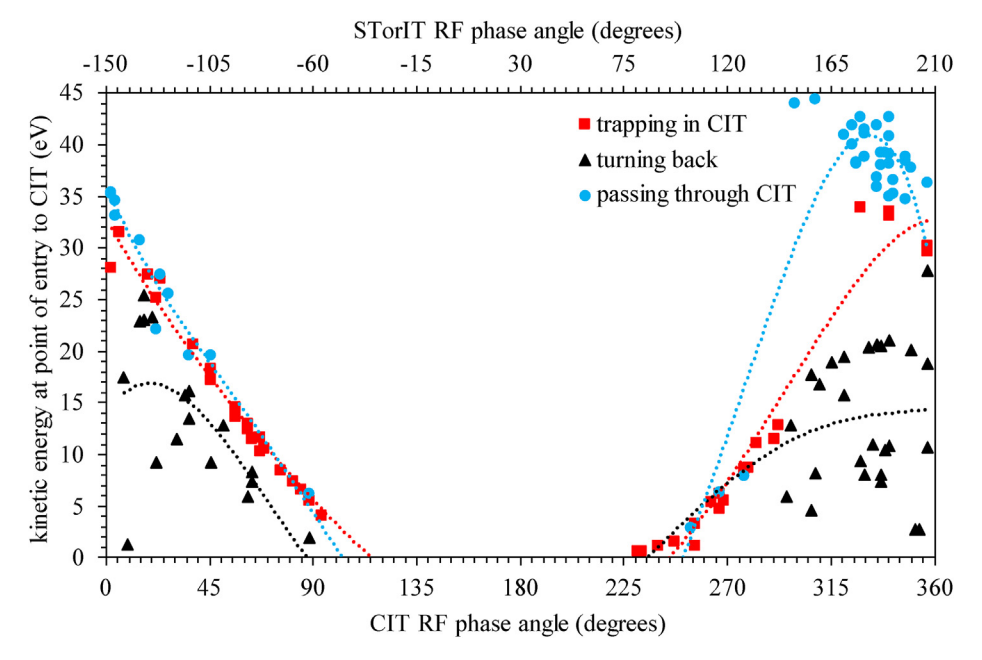


Fig. 6. Kinetic energies of ions that are trapped (red), pass through the CIT (blue), and turn back after entering the CIT (black). Forty-five ions are shown undergoing each outcome. The figure is not indicative of the actual percentages of ions displaying these three behaviors. The trendlines (dotted) are fitted to 5th order polynomials as a guide to the eye.

possesses insufficient kinetic energy to escape the STorIT. Immediately beyond the  $90^{\circ}-230^{\circ}$  range, ions exit the STorIT with relatively low kinetic energy which works in conjunction with the RF phase of the CIT to successfully decelerate and trap ions within the CIT, as indicated in Fig. 6. Most trapped ions enter the CIT as the RF pseudopotential well is on the rise, i.e. within the first and fourth quadrants, indicating that the CIT RF potential decelerates the ions.

The ions that traverse the CIT (blue) and those that turn back towards the STorIT (black) have kinetic energies on the high and low ends of the distribution respectively. Fig. 6 also suggests that the ideal kinetic energy for trapping is a function of the RF phase of the CIT. This observation in the current coaxial ion trap is consistent with the behavior of a 3D QIT during ion injection. Past studies have shown the existence of a single correct RF phase for any given kinetic energy of ion [7,28,29] and two possible RF phases in the presence of end-cap holes [26]. The correlation between the kinetic energy of trapped ions and RF phase seen in Fig. 6 is also corroborated by a study on ion injection in the 3D QIT, where the optimum phase of the RF was seen to vary linearly with ion velocity for ions injected radially through the ring electrode [29].

Ions passing through the CIT and ions turning back from the CIT, concentrated at the top and bottom of the chart between phase angles 290° and 360° of the CIT respectively, are evidently effects of the kinetic energy being mismatched to the RF phase. If the kinetic energy is too high, the passage of the ions through the CIT is too fast to encounter enough collisions for successful trapping [7], while if it is too low, the ions enter the CIT but turn back, unable to overcome the RF barrier of the CIT. The probabilistic mismatch in RF phase and kinetic energy of ejecting ions explains the relatively low trapping efficiencies seen during radial injection of ions both in the 3D QIT [26,27] and in the present study.

The kinetic energy of ions exiting the STorIT is a function of pressure as well as the RF and AC voltages applied to the STorIT. Unfortunately, since these parameters are interrelated as well as directly tied to other aspects of ion trap operation and performance, they cannot be adjusted freely to manipulate the kinetic energy of ions exiting the STorIT. For instance, the mass resolution and trapping efficiency depend on the pressure (one favorably, and the

other adversely), the mass range of the STorIT depends on the RF voltage, and ejection efficiency depends on the AC voltage. Therefore, successful operation of the coaxial ion trap involves finding optimized conditions of pressure and applied potentials for ion transfer and trapping. Attempting to increase the trapping efficiency by increasing pressure beyond this optimal value compromises the mass resolution of the transfer step.

## 3.7. Relative RF phase vs. trapping efficiency

A study of the RF phase of the CIT relative to the STorIT in aspect ratio 3 is shown in Fig. 7 below. Trapping efficiency was calculated from among the transferred ions without considering the ions that reflect back towards the STorIT. While trapping efficiency varies between 5 and 10% over most of the phase angles, it increases markedly between phase angles 130° and 160° (RF voltage of the CIT leading that of the STorIT). Fig. 8 shows the variation of the electric potential and the electric field with the relative RF phase of the CIT. The optimal phase angle depends on the RF amplitudes of the STorIT and CIT and should be re-optimized if these voltages are changed significantly.

Fig. 8 shows the electric potential and field across the simplified coaxial trap. At 150°, where the trapping efficiency was high, the electric potentials of the STorIT and CIT are arranged so as to facilitate ejection and trapping in the two regions respectively. This, combined with the compatibility of the phase angle with the kinetic energy (Fig. 7), explain the improvement in trapping efficiency between 130° and 160°.

With this information, we simulated and optimized the operating parameters for aspect ratio 3. Operating the STorIT at an RF frequency of 1.5 MHz and potential of 575  $V_{(0-p)}$  resulted in a LMCO of approximately 54 Da. The pressure was maintained at 3.75 mTorr to facilitate trapping of ions in the CIT. The CIT was operated at an RF frequency of 1.5 MHz and a potential of 1050  $V_{(0-p)}$ . An AC voltage of 2.5  $V_{(0-p)}$  at 108 kHz was applied for 100  $\mu$ s to resonantly excite ions of mass 219 Da. Lower voltages were not sufficient to overcome the RF barrier of the STorIT, making the transfer efficiency low, while at higher voltages the trapping efficiency

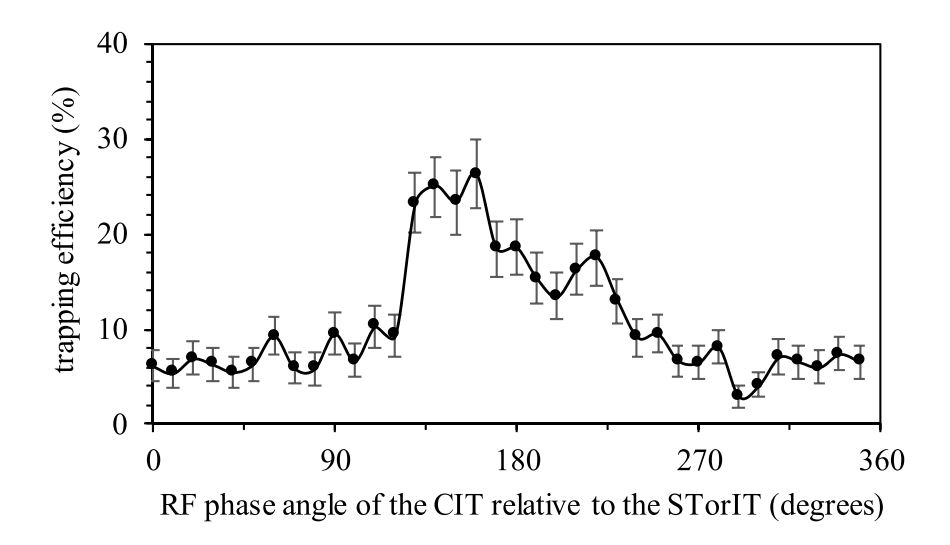


Fig. 7. RF phase vs trapping efficiency in aspect ratio 3 with RF voltages 575 V and 1050 V applied to the STorIT and CIT respectively. Each point consists of ions over the full distribution of kinetic energies.

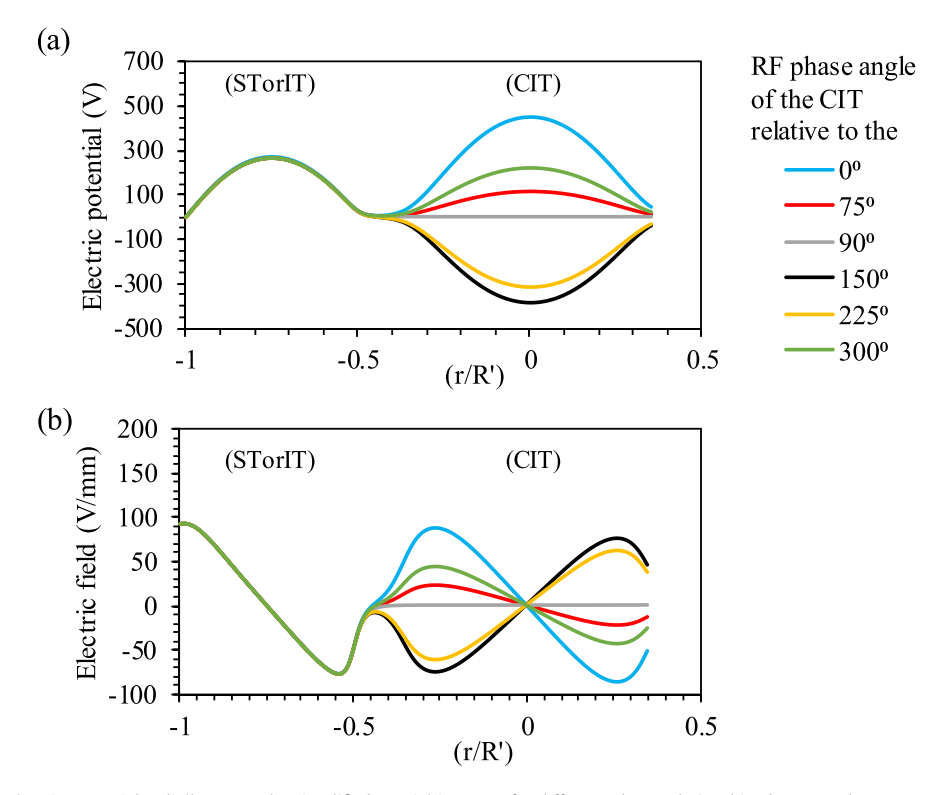


Fig. 8. (a) Variation of the electric potential radially across the simplified coaxial ion trap, for different phase relationships between the STorIT and CIT RF potentials. r/R' is the normalized radial distance along the trap. r/R' = -1 is the inner edge of AC<sub>Tor</sub>, while r/R' = 0.35 is the inner edge of the grounded electrode. (b) Variation of the electric field radially across the simplified coaxial ion trap.

suffered. This and other trends are indicated in the operating parameters in Table 1 below.

Experimenting with different  $RF_{Cyl}$  voltages added to the complexity of the conditions for ion ejection. Adjustments to the  $RF_{Cyl}$  voltage requires changes to the applied AC voltage in order to compensate for the change in the depth of the CIT pseudopotential well, as demonstrated in the data reported in Table 1. For example, from  $RF_{Cyl} = 800-1200\,V_{(0-p)}$  the number of transferred ions is seen

to correlate with the number of ions reflected back towards the STorIT and is attributed to the increased depth of the RF barrier within the CIT region. Consequently, the depth of the CIT pseudopotential well directly correlates with the fraction of ions being successfully trapped within the CIT. This intricate interplay between RF and AC voltage, pressure, transfer and trapping efficiency, and mass resolution contribute to the operational constraints of the coaxial ion trap.

**Table 1**The relationship between CIT RF voltage, AC voltage, and the number of ions transferred and trapped for aspect ratio 3 with pressure fixed at 3.75 mTorr and STorIT RF voltage of 575 V and 1.5 MHz. Each row indicates the percentage of ions transferred (does not include ions that enter CIT and turn back), ions trapped as a percentage of ions transferred, and the overall transfer efficiency out of 240 total ions.

CIT RF voltage (V)	Resonance AC voltage (V)	Ejection efficiency (%)	Trapping efficiency (%)	Overall transfer efficiency (%)
600	1.50	0.0	0.0	0.0
	1.75	9.6	0.0	0.0
	2.00	32.1	1.3	0.4
	2.50	62.9	2.0	1.2
	2.75	60.8	2.7	1.7
800	1.50	1.7	0.0	0.0
	1.75	9.6	13.0	1.2
	2.00	27.5	9.1	2.5
	2.50	59.2	6.3	3.8
	2.75	61.7	5.4	3.3
	3.00	71.7	7.0	5.0
1000	1.50	1.7	25.0	0.4
	1.75	11.2	14.8	1.7
	1.90	13.8	18.2	2.5
	2.00	22.5	20.4	4.6
	2.50	37.9	24.2	9.2
	2.75	48.8	20.5	10.0
	3.00	53.8	16.3	8.8
1200	1.50	0.4	0.0	0.0
	1.75	4.2	30.0	1.2
	2.00	9.6	17.4	1.7
	2.50	20.4	24.5	5.0
	2.75	21.7	25.0	5.4
	3.00	29.2	22.8	6.7

We adopted the approach of fixing the pressure based on the desired mass resolution, followed by determining the STorIT RF voltage based on the desired mass range. Once these parameters are fixed, the range CIT RF voltages which captures the chosen mass range is determined. Then an optimization similar to that done in Table 1 can help determine the combined CIT RF voltage and AC voltage in such a way that a satisfactory balance is achieved between transfer and trapping efficiencies.

Once ions are transferred to and trapped in the CIT, we skipped the step of collision-induced dissociation and performed fragment ion trapping in a separate step. The voltage of the CIT was lowered to 400 V to trap fragments of mass 50 m/z, and these could be selectively ejected through the holes in the end-cap electrodes using dipole resonant excitation with an AC voltage of 427 kHz and an amplitude of 2.4 V applied for 100 µsec to the end-caps superimposed on the RF voltage of the CIT. Forward or reverse scans are also expected to work as have been previously demonstrated in cylindrical traps.

## 4. Conclusion

In this work, we have investigated the key operation parameters of a simplified coaxial ion trap consisting of a STorIT and a CIT. Using select geometric parameters, the electric field of the STorIT can be adjusted to obtain optimum mass resolution and unidirectional ion ejection for a given aspect ratio. Consistent with previous simulation and experimental results on ion trap behavior, the mass resolution of the STorIT is optimal when the octopole term is small and positive and the radial inward ejection of ions was found to correlate with a positive hexapole term. Ensuring that both of these conditions are simultaneously met becomes difficult as the aspect ratio of the toroidal trap decreases. This limits the range of feasible aspect ratios and is the source of the main design constraint in the STorIT.

Mass selective ion ejection from toroidal to cylindrical traps was also demonstrated while retaining the remaining bulk ion population in the toroidal region. Mass transfer selectivity of the STorIT utilizing resonant mass ejection was observed to be relatively low.

Simulation of the simplified coaxial trap demonstrates that it is possible to transfer and trap ions from the STorIT to the CIT, albeit with significant ion losses in the current design. Examination of ejected ion kinetic energy and RF phase angle revealed that the ideal RF phase for trapping varies linearly with the kinetic energy. Ion loss during transfer as well as the correlation between RF phase and kinetic energy for trapping resemble the behavior of radially injected ions to a 3D quadrupole.

The transfer and trapping efficiency of ions depend on the RF voltages of both the STorIT and the CIT, RF phase of the CIT, amplitude of the resonant AC voltage, pressure, and kinetic energy of ions. Among these, the RF phase of the CIT was optimized to obtain the maximum possible trapping efficiency of transferred ions. However, most of these parameters have limited flexibility, being tied to other aspects of ion trap performance such as mass resolution and mass range.

Given that the trapping efficiency is affected by pressure, it is possible that experimenting with different background gases may be useful. Increasing the pressure compromises the selectivity of mass transfer from the STorIT. However, a heavier background gas may help with trapping efficiency at a lower pressure. Another likely solution may be the adoption of a technique similar to discontinuous pressure atmospheric inlet (DAPI) which may help to lower the kinetic energies of ions at the point of entry to the CIT, thereby lowering the pressure requirement for successful trapping of ions, ensuring that mass resolution is not compromised [32]. Also among the avenues for improvement of the coaxial ion trap is the possibility of operating in the digital mode which may help synchronize the STorIT and CIT better for improved transfer efficiency of ions [33]. There are other modes of operation available which were not explored in this work. For instance, the high kinetic energy of ions entering the CIT can be explained by the presence of a deeper pseudopotential well on the STorIT compared to the CIT. Therefore, by applying STorIT RF voltages to AC<sub>Tor</sub> and barrel electrodes instead of RF<sub>Tor</sub>, and by applying the CIT voltages to electrodes RF<sub>CvI</sub>, the pseudopotential well of the CIT becomes deeper than that of the STorIT which may also improve the trapping efficiency of ions.

The optimal operation of the coaxial ion trap is hinged on a number of trade-offs, and compromises between performance parameters become necessary based on the requirements of the application. These trade-offs govern the main operating constraints of the coaxial ion trap. The results from the study demonstrate how geometry and operating conditions can be manipulated to successfully perform tandem mass spectrometry in a coaxial ion trap.

## **Author statement**

**Radhya Gamage**: methodology, investigation, formal analysis, writing — original draft. **Praneeth Hettikankanange**: software, methodology. **Kyle Lyman**: resources. **Daniel Austin**: writing — review & editing, supervision. **Nicholas Taylor**: conceptualization, writing — review & editing.

## **Declaration of competing interest**

The authors declare that they have no known competing financial interests or personal relationships that could have appeared to influence the work reported in this paper.

## Acknowledgements

The authors thank the U.S. National Science Foundation for funding this work (awards 2003667 and 2003592).

#### References

- [1] Z. Ouyang, R. Cooks, Miniature mass spectrometers, Annu. Rev. Anal. Chem. 2 (1) (2009) 187–214.
- [2] E.R. Badman, R.G. Cooks, Miniature mass analyzers, J. Mass Spectrom. 35 (6) (2000) 659–671.
- [3] R.T. Short, D.P. Fries, M.L. Kerr, C.E. Lembke, S.K. Toler, P.G. Wenner, R.H. Byrne, Underwater mass spectrometers for in situ chemical analysis of the hydrosphere, J. Am. Soc. Mass Spectrom. 12 (6) (2001) 676–682.
- [4] R. Zou, W. Cao, L. Chong, W. Hua, H. Xu, Y. Mao, J. Page, R. Shi, Y. Xia, T.Y. Hu, W. Zhang, Z. Ouyang, Point-of-Care tissue analysis using miniature mass spectrometer, Anal. Chem. 91 (1) (2018) 1157–1163.
- [5] R. Arevalo, W. Brinckerhoff, F.V. Amerom, R. Danell, V. Pinnick, X. Li, S. Getty, L. Hovmand, A. Grubisic, P. Mahaffy, F. Goesmann, H. Steininger, Design and demonstration of the mars organic molecule analyzer (MOMA) on the Exo-Mars 2018 rover, in: IEEE Aerospace Conference, 2015.
- [6] P.E. Leary, G.S. Dobson, J.A. Reffner, Development and applications of portable gas chromatography-mass spectrometry for emergency responders, the military, and law-enforcement organizations, Appl. Spectrosc. 70 (5) (2016) 888–896
- [7] J.C. Schwartz, M.W. Senko, J.E.P. Syka, A two-dimensional quadrupole ion trap mass spectrometer, J. Am. Soc. Mass Spectrom. 13 (2002) 659–669.
- [8] M. Welling, H. Schuessler, R. Thompson, H. Walther, Ion/molecule reactions, mass spectrometry and optical spectroscopy in A linear ion trap, Int. J. Mass Spectrom. Ion Process. 172 (1–2) (1998) 95–114.
- [9] J.A. Hager, New linear ion trap mass spectrometer, Rapid Commun. Mass Spectrom. 16 (6) (2002) 512–526.
- [10] Z. Ouyang, G. Wu, Y. Song, H. Li, W.R. Plass, R.G. Cooks, Rectilinear ion trap: concepts, calculations, and analytical performance of a new mass analyzer, Anal. Chem. 76 (16) (2004) 4595–4605.
- [11] D. Church, Storage-ring ion trap derived from the linear quadrupole radio-

- frequency mass filter, J. Appl. Phys. 40 (8) (1969) 3127–3134.
- [12] I. Waki, S. Kassner, G. Birkl, H. Walther, Observation of ordered structures of laser-cooled ions in A quadrupole storage ring, Phys. Rev. Lett. 68 (13) (1992) 2007–2010.
- [13] M. Aramaki, Y. Sakawa, T. Shoji, New method of particle confinement time measurement in RF traps, Jap. J. Appl. Phys. 39 (Part 2) (2000) L246–L248. No. 3A/B.
- [14] S.Á. Lammert, W.R. Plass, C.V. Thompson, M.B. Wise, Design, optimization and initial performance of a toroidal rf ion trap mass spectrometer, Int. J. Mass Spectrom. 212 (2001) 25–40.
- [15] N. Taylor, D. Austin, A simplified toroidal ion trap mass analyzer, Int. J. Mass Spectrom. 321–322 (2012) 25–32.
- [16] P.M. Hettikankanange, D.E. Austin, Varying the aspect ratio of toroidal ion traps: implications for design, performance, and miniaturization, Int. J. Mass Spectrom. 470 (2021), 116703.
- [17] Y. Peng, B.J. Hansen, H. Quist, Z. Zhang, M. Wang, A.R. Hawkins, D.E. Austin, Coaxial ion trap mass spectrometer: concentric toroidal and quadrupolar trapping regions, Anal. Chem. 83 (14) (2011) 5578–5584.
- [18] Q. Yu, L. Tang, K. Ni, X. Qian, X. Wang, Computer simulations of a new toroidal-cylindrical ion trap mass analyzer, Rapid Commun. Mass Spectrom. 30 (20) (2016) 2271–2278.
- [19] H. Yang, C. Xu, L. Yue, S. Mikhail, Y. Pan, C. Ding, Optimization of performance of toroidal ion trap with trianglar electrode by theoretical simulation, Chin. J. Anal. Chem. 44 (3) (2016) 482–488.
- [20] M. Jahandar Lashaki, M. Fayaz, S. Niknaddaf, Z. Hashisho, Effect of the adsorbate kinetic diameter on the accuracy of the Dubinin–Radushkevich equation for modeling adsorption of organic vapors on activated carbon, J. Hazard Mater. 241–242 (2012) 154–163.
- [21] J.M. Wells, E.R. Badman, R.G. Cooks, A quadrupole ion trap with cylindrical geometry operated in the mass-selective instability mode, Anal. Chem. 70 (3) (1998) 438–444.
- [22] A. Makarov, Resonance ejection from the Paul trap: a theoretical treatment incorporating a weak octapole field, Anal. Chem. 68 (23) (1996) 4257–4263.
- [23] Q. Dang, F. Xu, X. Huang, X. Fang, R. Wang, C. Ding, Linear ion trap with added octopole field component: the property and method, J. Mass Spectrom. 50 (12) (2015) 1400–1408.
- [24] J. Franzen, R.-H. Gabling, M. Schubert, Y. Wang, Nonlinear Ion Traps. Practical Aspects of Ion Trap Mass Spectrometry, vol. I, CRC Press, Inc., 1995 pp 49 –167
- [25] G. Wu, R. Cooks, Z. Ouyang, Geometry optimization for the cylindrical ion trap: field calculations, simulations and experiments, Int. J. Mass Spectrom. 241 (2–3) (2005) 119–132.
- [26] S. Quarmby, R. Yost, Fundamental studies of ion injection and trapping of electrosprayed ions on a quadrupole ion trap, Int. J. Mass Spectrom. 190–191 (1999) 81–102.
- [27] S. Mcluckey, G. Glish, K. Asano, Coupling of an atmospheric-samling ion source with an ion-trap mass spectrometer, Anal. Chim. Acta 225 (1989) 25–25
- [28] C. Weil, M. Nappi, C. Cleven, H. Wollnik, R. Cooks, Multiparticle simulation of ion injection into the quadrupole ion trap under the influence of helium buffer gas using short injection times and DC pulse potentials, Rapid Commun. Mass Spectrom. 10 (7) (1996) 742–750.
- [29] O. Chun-Sing, H. Schuessler, Confinement of ions created externally in A radio-frequency ion trap, J. Appl. Phys. 52 (3) (1981) 1157–1166.
- [30] G. Dolnikowski, M. Kristo, C. Enke, J. Watson, Ion-trapping technique for ion/molecule reaction studies in the center quadrupole of a triple quadrupole mass spectrometer, Int. J. Mass Spectrom. Ion Process. 82 (1–2) (1988) 1–15.
- [31] L. Li, X. Zhou, J. Hager, Z. Ouyang, High efficiency tandem mass spectrometry analysis using dual linear ion traps, Analyst 139 (19) (2014) 4779–4784.
- [32] L. Gao, R. Cooks, Z. Ouyang, Breaking the pumping speed barrier in mass spectrometry: discontinuous atmospheric pressure interface, Anal. Chem. 80 (11) (2008) 4026–4032.
- [33] L. Ding, M. Sudakov, F. Brancia, R. Giles, S. Kumashiro, A digital ion trap mass spectrometer coupled with atmospheric pressure ion sources, J. Mass Spectrom. 39 (5) (2004) 471–484.